

## Supporting Information

### Boron difluoride formazanates with thiophene and 3,4-ethylenedioxythiophene capping and their electrochemical polymerization

Chandan Kumar, Abhijeet R. Agrawal, Nani Gopal Ghosh, Himadri S. Karmakar, Sarasija Das, Neha Rani Kumar, Vishal W. Banewar<sup>b\*</sup> and Sanjio S. Zade<sup>a\*</sup>

<sup>a</sup>Department of Chemical Sciences, Indian Institute of Science Education and Research (IISER) Kolkata, Mohanpur-741246, INDIA

<sup>b</sup>Department of Chemistry, Institute of Science, 15-Madam Cama Road, Fort- Mumbai (Maharashtra)-400032, INDIA.

Email: sanjiozade@iiserkol.ac.in, banewar@iscm.ac.in

#### Table of Contents

Contents	Page No
General procedure	S2-S3
Synthesis	S3-S5
<b>Fig. S1</b> Crystal packing structure of <b>9</b>	S6
<b>Table S1</b> Crystal data of Complex <b>9</b>	S7
<b>Table S2</b> Orbital picture generated by DFT at B3LYP/6-31G(d) level compound <b>8</b> and <b>9</b>	S8
<b>Fig. S2</b> Charge transport pathways for compound <b>9</b>	S9
<b>Table S3</b> Calculation of hole mobility compound <b>9</b>	S10
<b>Table S4</b> Optoelectronic properties of compound <b>7-9</b> and <b>Fig. S3</b> spectroelectrochemistry of <b>P2</b>	S10
<b>Fig. S4</b> <sup>1</sup> H NMR and <b>Fig. S5</b> <sup>13</sup> C NMR of compound <b>6</b>	S11
<b>Fig. S6</b> <sup>1</sup> H NMR and <b>Fig. S7</b> <sup>13</sup> C NMR of compound <b>7</b>	S12
<b>Fig. S8</b> <sup>1</sup> H NMR and <b>Fig. S9</b> <sup>13</sup> C NMR of compound <b>8</b>	S13
<b>Fig. S10</b> <sup>1</sup> H NMR and <b>Fig. S11</b> <sup>13</sup> C NMR of compound <b>9</b>	S14
References	S15

## General measurement and characterization

All commercially available chemicals and reagents were purchased and used without further purification unless otherwise mentioned. Solvents like toluene and THF were distilled from sodium/benzophenone before used and stored under nitrogen. All air and water sensitive reactions were performed in oven-dried glassware using standard Schlenk techniques. 2-bromothiophene, EDOT, tributyltinchloride ( $\text{Bu}_3\text{SnCl}$ ),  $\text{Pd}(\text{PPh}_3)_4$  were purchased from Spectrochem and  $\text{TBAPF}_6$  was purchased from Aldrich and used without further purification. *n*-BuLi (1.6 M in hexane) was purchased from Spectrochem. Reactions were monitored by thin layer chromatography (TLC) using Merck plates (TLC Silica Gel 60 F254). Developed TLC plates were observed under ultraviolet light (254 nm/366 nm). Silica gel (Merck) was used for column chromatography.  $^1\text{H}$  NMR and  $^{13}\text{C}$  NMR spectra of the compounds were recorded using a JEOL ECS 400 MHz and Bruker 500 MHz spectrometer with  $\text{CDCl}_3$  as the solvent, and Chemical shifts ( $\delta$ ) are reported in ppm and were referenced to the residual undeuterated solvent signal as an internal reference ( $\text{CDCl}_3$ , 7.26 ppm for  $^1\text{H}$  and 77.23 ppm for  $^{13}\text{C}$ ).  $^{11}\text{B}$  spectra were referenced to  $\text{BF}_3\cdot\text{OEt}_2$  at 0 ppm, and  $^{19}\text{F}$  NMR spectra were referenced to  $\text{CFCl}_3$  (0 ppm), Coupling constants ( $J$ ) are given in Hz and the apparent resonance multiplicity is reported as s (singlet), d (doublet), dd (doublet of doublets), t (triplet), q (quartet), m (multiplet). UV-vis absorption spectrum was recorded on a JASCO V-670 spectrophotometer. HRMS data were collected using maXis impact BRUKER ESI-MS instrument.

Cyclic voltammetry was performed at room temperature using dry acetonitrile as solvent, tetrabutylammoniumhexafluorophosphate ( $\text{TBAPF}_6$ ) as supporting electrolyte at a scan rate of 100 mV/s under nitrogen atmosphere. A platinum disk was used as working electrode, platinum wire was used as counter electrode and silver wire was used as pseudo reference electrode. The potential was externally calibrated after each experiment, against the ferrocene/ferrocenium couple.

Electrochemical studies were performed using a Princeton Applied Research 263A potentiostat using a platinum (Pt) disk electrode as the working electrode, a platinum wire as the counter electrode, and an Ag wire as the reference electrode. Nonaqueous  $\text{Ag}/\text{Ag}^+$  wire was prepared by dipping silver wire in a solution of  $\text{FeCl}_3$  and HCl. Pt disk electrodes were polished with gamma alumina and washed with water and acetone and were dried with nitrogen gas before use to eliminate any incipient oxygen. The polymer films were deposited on ITO-coated glass electrodes with dimensions of  $5 \times 0.7 \text{ cm}^2$ . Before examining the optical properties of the polymer films, the films were rinsed with ACN. The UV-vis-near infrared (NIR) spectra were carried out using a HITACHI

U-4100 UV-vis-NIR spectrophotometer. All electrochemical potentials were reported against Ag/Ag<sup>+</sup> taking ferrocene as the external standard; the  $E^{1/2}_{\text{ferrocene}}$  is +0.37 V.

## Synthesis and Characterisation of compounds

### Synthesis of triaryl formazan **6**<sup>1-3</sup>

4-Bromophenylhydrazine hydrochloride (2.23g, 10 mmol) was dissolved in ethanol (20 ml) with triethylamine (2.8 ml, 20 mmol) and ethanol. After the mixture was stirred for 30 min, benzaldehyde (1.06 ml, 10 mmol) was added and the mixture was allowed to stir for additional 1 h. To this reaction mixture sodium carbonate hydrated (3.6 g, 34 mmol), tetrabutylammonium bromide (TBAB) (0.32 g, 0.1 mmol), water (50 ml), and dichloromethane (50 ml) were added and stirred at 0°C for another 1 h. In a separate flask 4-bromoaniline (1.72 g, 10 mmol), and concentrated HCl (10 ml) were mixed in water (10 ml) and cooled in an ice bath. An ice-cold solution of sodium nitrite (0.7 g, 12 mmol), in water (10 ml) was then slowly added to the aniline solution over a period of 30 minutes. This diazonium salt solution was then added dropwise to the hydrazine mixture. After addition, the organic phase in the biphasic reaction turned deep red color. After stirring for 2 h at room temperature, the organic layer was collected and washed with water (500 ml) in a funnel. The aqueous layer was extracted with an additional 20 ml dichloromethane. Then the organic layer was dried over Na<sub>2</sub>SO<sub>4</sub> and the solution was taken to dryness on a rotary evaporator after filtration. The solid was dissolved in boiling methanol followed by cooling to furnish a dark red compound **6** microcrystalline solid 3.69 g, 62% yield. <sup>1</sup>H NMR δ<sub>H</sub> (400 MHz, CDCl<sub>3</sub>) 15.24 (1 H, s), 8.08 (2 H, d, *J* 7.6 Hz), 7.56 (8 H, d, *J* 3.2 Hz), 7.45 (2 H, t, *J* 7.6 Hz), 7.37 (1 H, t, *J* 7.2 Hz). <sup>13</sup>C NMR δ<sub>C</sub> (126 MHz, CDCl<sub>3</sub>) 146.9, 141.7, 137.1, 132.8, 128.7, 128.2, 126.1, 121.3, 120.4.

HRMS (ESI) : Calc. for C<sub>19</sub>H<sub>14</sub>Br<sub>2</sub>N<sub>4</sub> [M+H]<sup>+</sup> 456.9663; found: 456.9433.

### Synthesis of formazan-BF<sub>2</sub> complex **7**

Formazan **6** (458.15 mg, 1 mmol), was dissolved in dry toluene. Triethylamine (0.42 mL, 4 mmol) was then added to this solution slowly and the solution was stirred for 10 min before BF<sub>3</sub>·Et<sub>2</sub>O (1 mL, 6 mmol) was added and the solution was heated with stirring at 80°C for 18 h. The solution gradually turned from dark red to dark purple during this time. After completion of reaction, the reaction mixture was quenched with 20 ml deionized water. The organic layer was dried over Na<sub>2</sub>SO<sub>4</sub>, gravity filtered and concentrated in vacuo. The crude product was purified by silica gel column chromatography eluting with hexane/dichloromethane (95:5) to produce compound **7** as a dark purple solid (205 mg, 41% yield). <sup>11</sup>B NMR δ<sub>B</sub> (161 MHz, CDCl<sub>3</sub>) -0.62 (t, *J* 29.4 Hz).

$^1\text{H}$  NMR  $\delta_{\text{H}}$  (400 MHz,  $\text{CDCl}_3$ ) 8.07 (2 H, dd,  $J$  8.1 Hz, 1.5 Hz), 7.79 (4 H, d,  $J$  8.8 Hz), 7.62 (4 H, d,  $J$  8.9 Hz), 7.47 (3 H, t,  $J$  7.8 Hz).  $^{19}\text{F}$  NMR  $\delta_{\text{F}}$  (471 MHz,  $\text{CDCl}_3$ ) -143.13 (q,  $J$  29 Hz).

$^{13}\text{C}$  NMR  $\delta_{\text{C}}$  (126 MHz,  $\text{CDCl}_3$ ) 149.4, 142.9, 133.3, 132.5, 129.8, 129.0, 125.7, 124.9, 124.5.

HRMS (ESI): Calc. for  $\text{C}_{19}\text{H}_{13}\text{BBr}_2\text{F}_2\text{N}_4$   $[\text{M}+\text{H}]^+$  504.9646; found: 504.9628.

2-Tributylstannylthiophene and 2-(Tributylstannyl)-3,4-(ethylenedioxy)thiophene were synthesized by previously published procedure respectively.<sup>4,5</sup>

### Synthesis of thiophene coupled formazan- $\text{BF}_2$ complex **8**<sup>6</sup>

In a 100 mL three neck round bottomed flask under nitrogen atmosphere Formazanate- $\text{BF}_2$  complex **7** (101.19 mg, 0.20 mmol), 2-tributylthienyltin (149.27 mg, 0.40 mmol) in dry toluene. The reaction mixture was purged with nitrogen for 15 minutes then  $\text{Pd}(\text{PPh}_3)_4$  (23.11 mg, 0.02 mmol) was added and the reaction mixture was refluxed for overnight. After completion of reaction solvent was evaporated and the desired compound was isolated by silica gel column chromatography with hexane/dichloromethane (90:10) to yield **8** as purple/blue solid (84%).  $^{11}\text{B}$  NMR  $\delta_{\text{B}}$  (161 MHz,  $\text{CDCl}_3$ ) -0.45 (t,  $J$  29.5 Hz).  $^1\text{H}$  NMR  $\delta_{\text{H}}$  (500 MHz,  $\text{CDCl}_3$ ) 8.13 (2 H, d,  $J$  7.2 Hz), 7.97 (4 H, d,  $J$  8.5 Hz), 7.72 (4 H, d,  $J$  8.7 Hz), 7.50 (3 H, t,  $J$  7.3 Hz), 7.42 (2 H, d,  $J$  3.5 Hz), 7.36 (2 H, d,  $J$  4.6 Hz), 7.17 – 7.09 (2 H, m).

$^{13}\text{C}$  NMR  $\delta_{\text{C}}$  (126 MHz,  $\text{CDCl}_3$ ) 143.2, 135.9, 133.9, 129.5, 129.0, 128.6, 126.5, 126.4, 125.7, 124.5, 124.1.  $^{19}\text{F}$  NMR  $\delta_{\text{F}}$  (471 MHz,  $\text{CDCl}_3$ ) -143.27 (q,  $J$  29.3 Hz).

HRMS (ESI): Calc. for  $\text{C}_{27}\text{H}_{19}\text{BF}_2\text{N}_4\text{S}_2$   $[\text{M}+\text{H}]^+$  513.1190; found: 513.1168.

### Synthesis of EDOT coupled formazan- $\text{BF}_2$ complex **9**<sup>6</sup>

In a 100 mL three neck round bottomed flask under nitrogen atmosphere Formazanate- $\text{BF}_2$  complex **7** (101.19 mg, 0.20 mmol), EDOT-2-tributylthienyltin (172.8 mg, 0.40) in dry toluene. The reaction mixture was purged with nitrogen for 15 minutes then  $\text{Pd}(\text{PPh}_3)_4$  (23.11 mg, 0.02 mmol) was added and the reaction mixture was refluxed for overnight. After completion of reaction solvent was evaporated and the desired compound was isolated by silica gel column chromatography with hexane/dichloromethane (90:10) to yield **9** as purple/blue solid (75%).

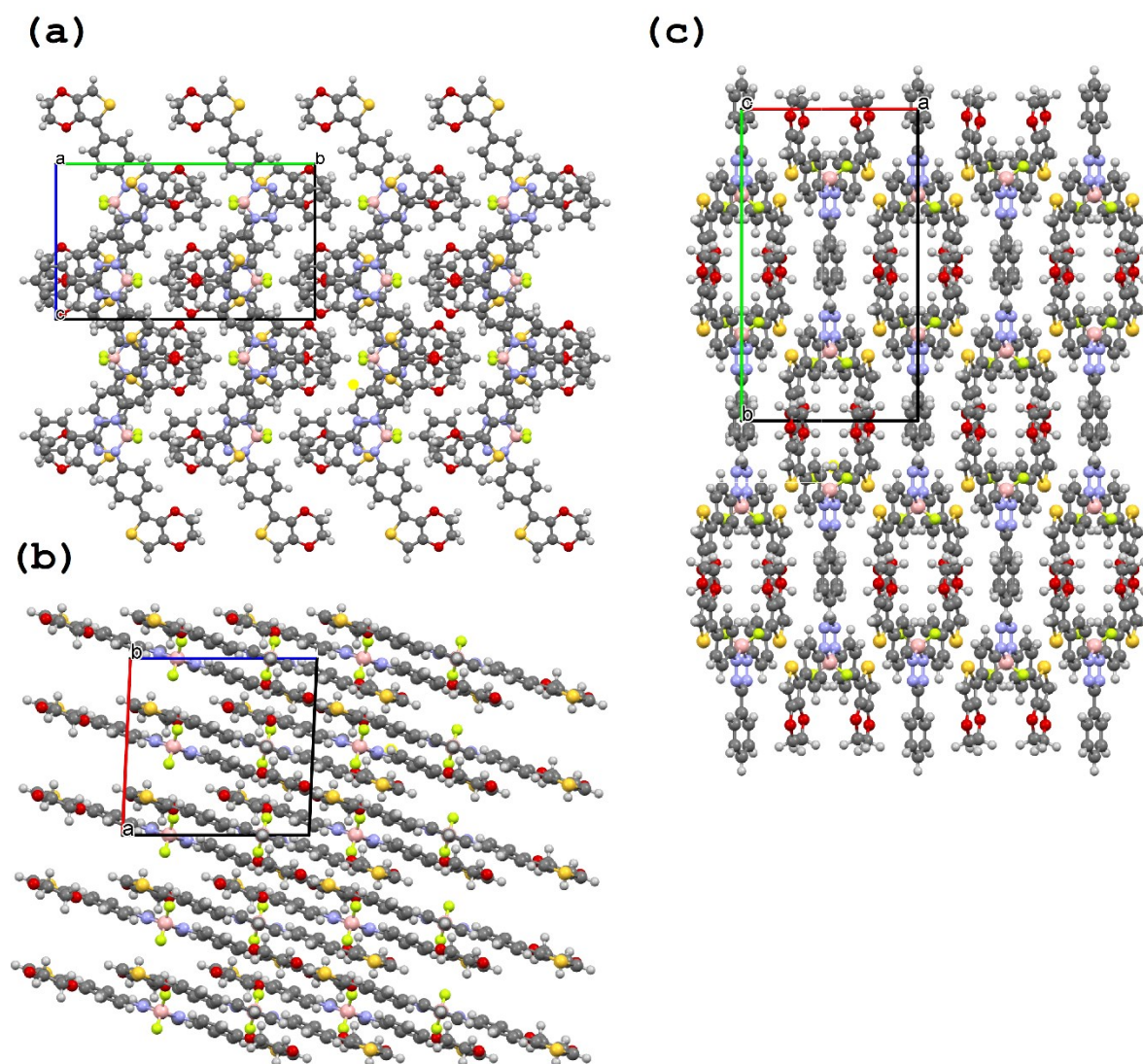
$^1\text{H}$  NMR  $\delta_{\text{H}}$  (500 MHz,  $\text{CDCl}_3$ ) 8.13 (2 H, d,  $J$  7.3 Hz), 7.95 (4 H, d,  $J$  8.1 Hz), 7.83 (2 H, d,  $J$  8.4 Hz), 7.47 (3 H, t, 7.4 Hz), 6.38 (2 H, s), 4.35 (2 H, s), 4.27 (2 H, s).

$^{13}\text{C}$  NMR  $\delta_{\text{C}}$  (126 MHz,  $\text{CDCl}_3$ ) 142.6, 142.4, 139.7, 134.9, 134.2, 129.3, 128.9, 126.4, 125.7, 123.7, 116.8, 99.5, 65.1, 64.6.  $^{19}\text{F}$  NMR  $\delta_{\text{F}}$  (471 MHz,  $\text{CDCl}_3$ ) -142.77(q,  $J$  29.3 Hz).

HRMS (ESI): Calc. for  $\text{C}_{31}\text{H}_{23}\text{BF}_2\text{N}_4\text{O}_4\text{S}_2$   $[\text{M}+\text{H}]^+$  629.1300; found: 629.1297.

## X-ray Crystallography

The structural analysis which was carried out for of the compound **9** reveals that the molecule crystallises in monoclinic crystal system with a space group C2/c with half a molecule in the asymmetric unit (Fig. S1). The solid-state structures of **9** confirm the presence of four coordinate boron, bound to the formazanate backbone through two nitrogen atoms. Single crystals of compound **9** was diffracted on Dual, Cu at zero, Eos diffractometer. The crystals were solved using Olex2,<sup>7</sup> and refined with the ShelXL refinement package using Least Squares minimization.<sup>8</sup> CCDC no. of crystal is 2005714.

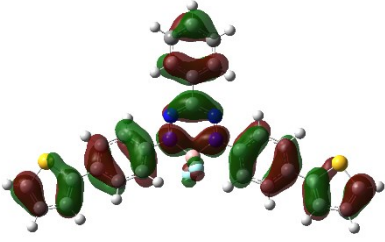
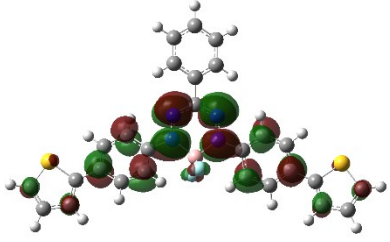
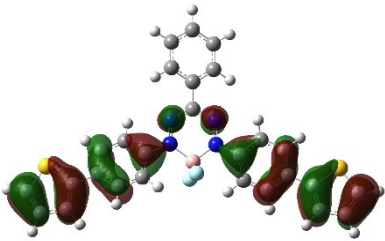
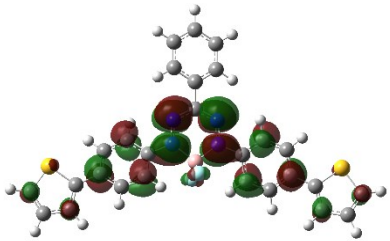
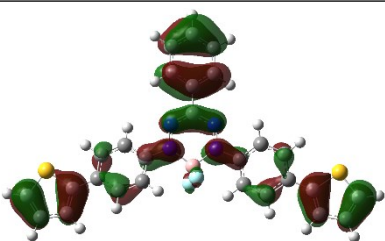
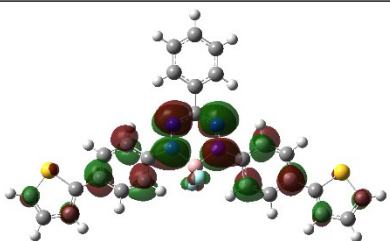


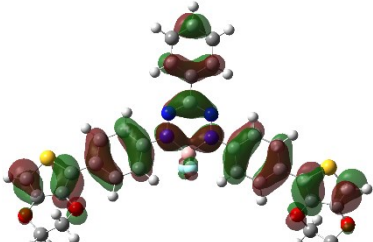
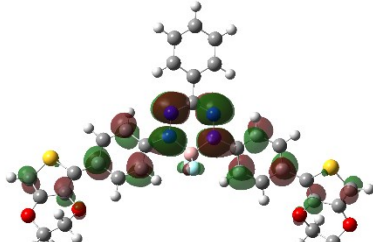
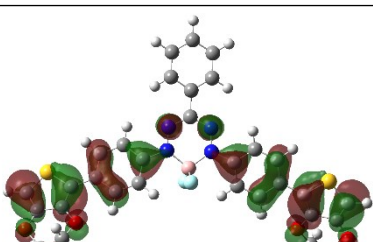
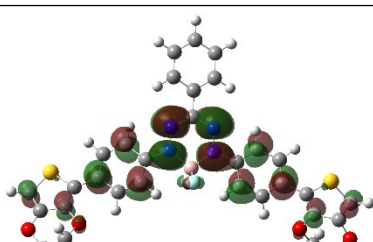
**Fig. S1** Crystal packing structure of **9**

**Table S1** Crystal data and structure refinement for complex **9**.

Empirical formula	C <sub>31</sub> H <sub>19</sub> BF <sub>2</sub> N <sub>4</sub> O <sub>4</sub> S <sub>2</sub>
Formula weight	624.43
Temperature/K	100.00
Crystal system	monoclinic
Space group	C2/c
a/Å	11.4090(3)
b/Å	20.0988(5)
c/Å	12.0473(2)
α/°	90.00
β/°	92.607(2)
γ/°	90.00
Volume/Å <sup>3</sup>	2759.68(12)
Z	4
ρ <sub>calc</sub> /g/cm <sup>3</sup>	1.503
μ/mm <sup>-1</sup>	2.273
F(000)	1280.0
Crystal size/mm <sup>3</sup>	0.25 × 0.15 × 0.1
Radiation	CuKα (λ = 1.54184)
2θ range for data collection/°	8.8 to 132.36
Index ranges	-9 ≤ h ≤ 13, -23 ≤ k ≤ 22, -14 ≤ l ≤ 14
Reflections collected	9232
Independent reflections	2414 [R <sub>int</sub> = 0.0229, R <sub>sigma</sub> = 0.0202]
Data/restraints/parameters	2414/0/201
Goodness-of-fit on F <sup>2</sup>	1.062
Final R indexes [I ≥ 2σ (I)]	R <sub>1</sub> = 0.0470, wR <sub>2</sub> = 0.1381
Final R indexes [all data]	R <sub>1</sub> = 0.0498, wR <sub>2</sub> = 0.1413

**Table S2** Orbital picture generated by DFT at B3LYP/6-31G(d) level compound **8** and **9**.

State	Compound <b>8</b>		Filled orbital	Empty orbital
S1	Excitation	H→L (100%)		
	$E_g$ (eV)	2.04		
	$\lambda$ (nm)	608		
	$f$	0.8764		
S2	Excitation	H-1→L (98%)		
	$E_g$ (eV)	2.60		
	$\lambda$ (nm)	476		
	$f$	0.0918		
S3	Excitation	H-2→L (96%)		
	$E_g$ (eV)	2.74		
	$\lambda$ (nm)	455		
	$f$	0.0449		

State	Compound <b>9</b>		Filled orbital	Empty orbital
S1	Excitation	H→L (100%)		
	$E_g$ (eV)	1.94		
	$\lambda$ (nm)	638		
	$f$	0.9577		
S2	Excitation	H-1→L (98%)		
	$E_g$ (eV)	2.46		
	$\lambda$ (nm)	505		
	$f$	0.1094		



**Computational Details:** All the calculations were performed using Gaussian16<sup>9</sup> suite of programs. The geometries of compound **9** in neutral and cationic states were fully optimized at B3LYP/6-31g(d) level. The reorganization energies were calculated at B3LYP/6-31g(d) level with the adiabatic potential energy surface. The transfer integrals for the different charge hopping pathways in the crystal structure were done at PW91PW91/6-31g(d) level by the site energy corrected method<sup>10,11</sup> and using AOMix program.<sup>12</sup> The PW91PW91 functional has been successfully employed for the calculations of transfer integrals.<sup>13</sup> The dimers for the calculations were extracted from the crystal structure of compound **9** (Fig. S2).

The charge carrier mobility,  $\mu$ , has been computed according to hopping model and is expressed as

$$\mu = \frac{e}{k_B T} D; \quad D = \frac{1}{2n} \sum_i d_i^2 k_i P_i$$

where  $D$  is diffusion coefficient,  $e$  is the electronic charge,  $k_B$  is Boltzmann constant,  $T$  is the temperature (298 K),  $d_i$  is centroid to centroid distance between the  $i$ th molecule and its neighbor,  $k_i$  is the hopping rate,  $n$  is the spatial dimensionality and  $P_i = k_i / \sum k_i$  is the probability of the charge transfer to the  $i$ th pathway.

The charge hopping rate for each hopping event can be expressed by Marcus-Hush equation<sup>14,15</sup>

$$k = \frac{4\pi^2}{h} \frac{1}{\sqrt{4\pi\lambda k_B T}} t^2 \exp\left[-\frac{\lambda}{4k_B T}\right]$$

where  $h$  is Planck constant,  $\lambda$  is internal reorganization energy, and  $t$  is transfer integral between the molecules in dimer.

The hole reorganization energies of the compounds were calculated according to the following equation:

$$\lambda = [E^0 M^+ - E^0 M^0] + [E^+ M^0 - E^+ M^+]$$

where  $E^0 M^0$  and  $E^+ M^+$  are the ground state energies of the neutral and cationic species, respectively;  $E^0 M^+$  is the energy of the neutral molecule at the cation geometry and  $E^+ M^0$  is the energy of cation at the neutral state geometry.

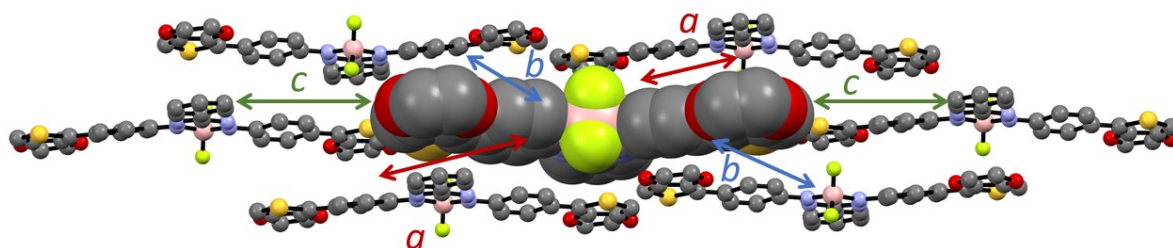


**Fig. S2** Charge transport pathways for compound **9** showing central molecule in spacifill model.

**Table S3** Calculated reorganization energies ( $\lambda$ ), distance ( $d$ ) between the Monomers for different pathways (as shown Fig. S2) and the corresponding transfer integrals ( $t$ ), and average hole mobilities ( $\mu$ )

$\lambda$ (eV)		Pathway	$d$ (Å)	$t$ (meV)		$\mu$ (cm <sup>2</sup> V <sup>-1</sup> s <sup>-1</sup> )	
hole	electron			hole	electron	hole	electron
0.276	0.366	a	12.047	-36	5	0.258	0.022
		b	8.34	-3	25		
		c	18.804	2	1		

**Table S4** Optoelectronic properties of 7-9

Compound	$\lambda_{max,ab}$ (nm)	$\lambda_{max,em}$ (nm)	Stokes shift ( $\nu_{ST}$ , cm <sup>-1</sup> )	$\epsilon$ (M <sup>-1</sup> cm <sup>-1</sup> )	$E_{HOMO}^{opt-LUMO}$ (eV)	$E_{ox,peak}$ (V)	$E_{ox,onset}$ (V)	$E_{HOMO}$ (eV)	$E_{LUMO}$ (eV)
7	520	648	3798	15941	2.00	1.70	1.53	-	-
8	570	736	3956	20511	1.80	1.79	1.47	-	-
9	606	786	3779	31034	1.70	1.78	1.46	-	-

$$E_{HOMO} = -(E_{ox,onset} + 4.8 - E_{(Fc/Fc^+,onset)}), \quad E_{(Fc/Fc^+,onset)} = 0.33 \text{ V}$$

$$E_{LUMO} = E_{HOMO} - E_{HOMO-LUMO}^{opt}, \quad E_{HOMO-LUMO}^{opt} = 1240/\lambda_{onset}$$

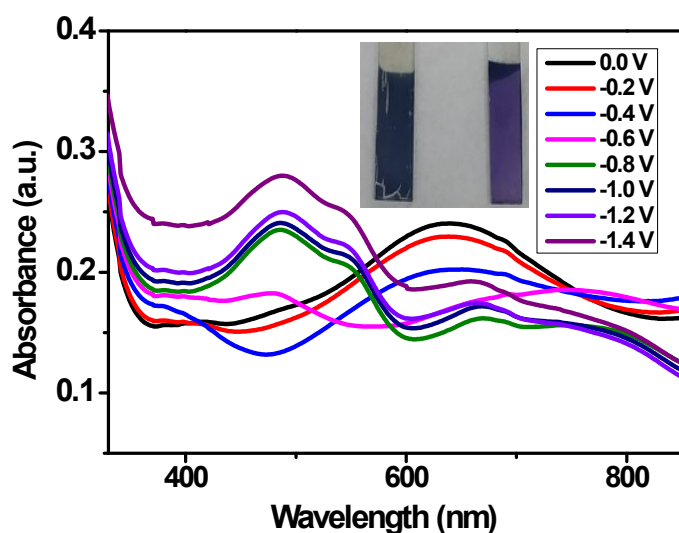


**Fig. S3** Spectroelectrochemistry of P2 thin films prepared on ITO-coated glass as a function of applied potential between 0.0 V and -1.4 V in ACN.

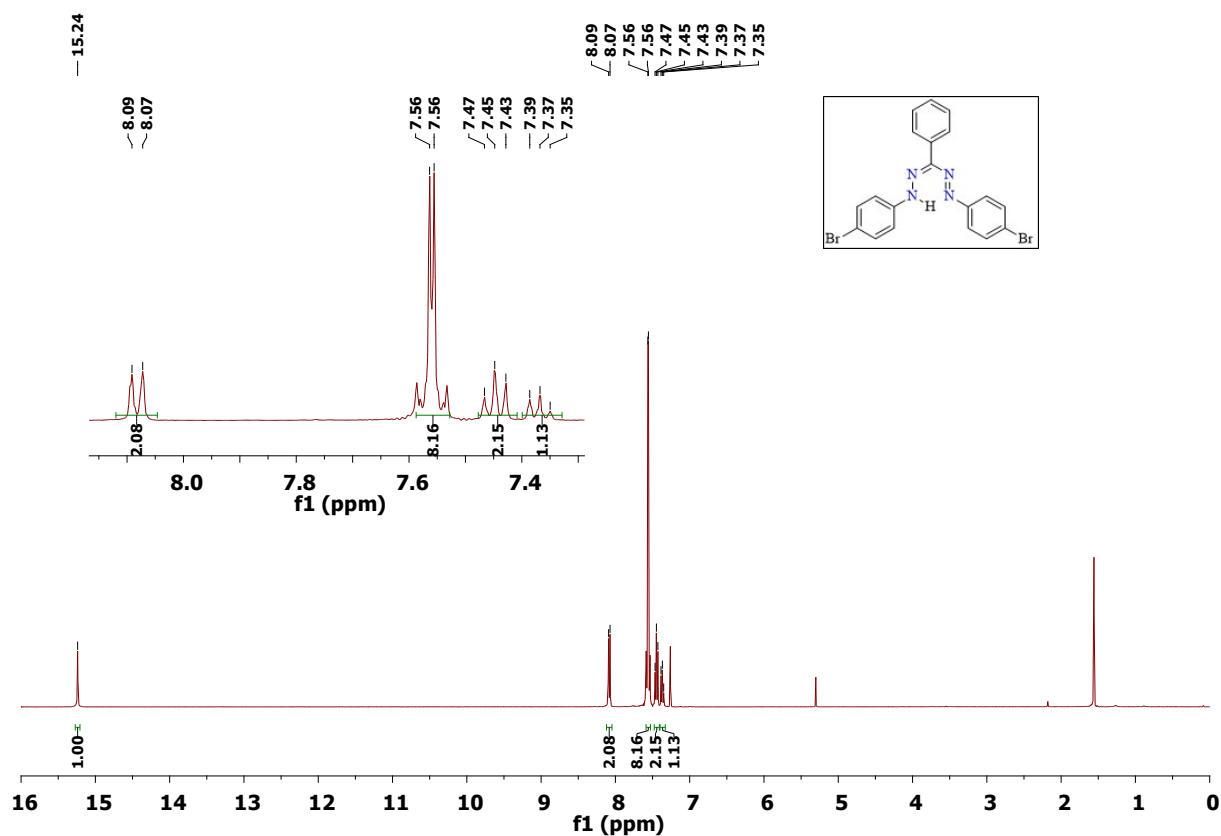
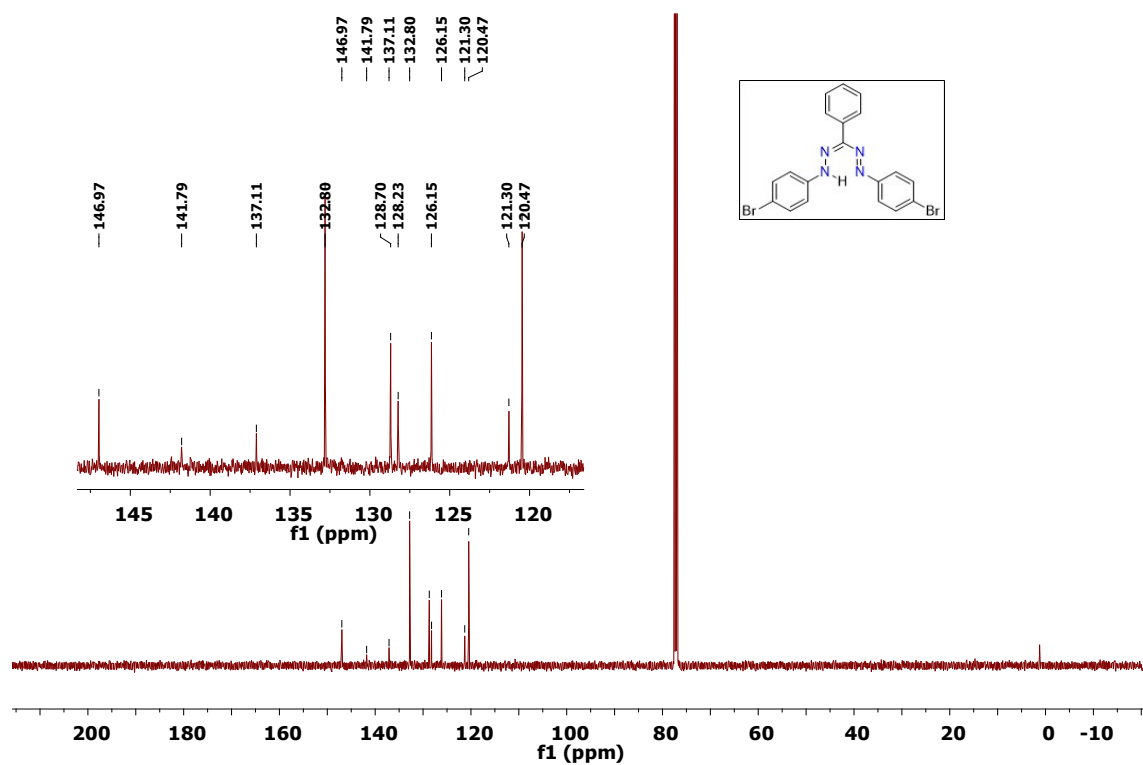


Fig. S4  $^1\text{H}$  NMR spectra of compound 6



S5  $^{13}\text{C}$  NMR spectra of compound 6

Fig.

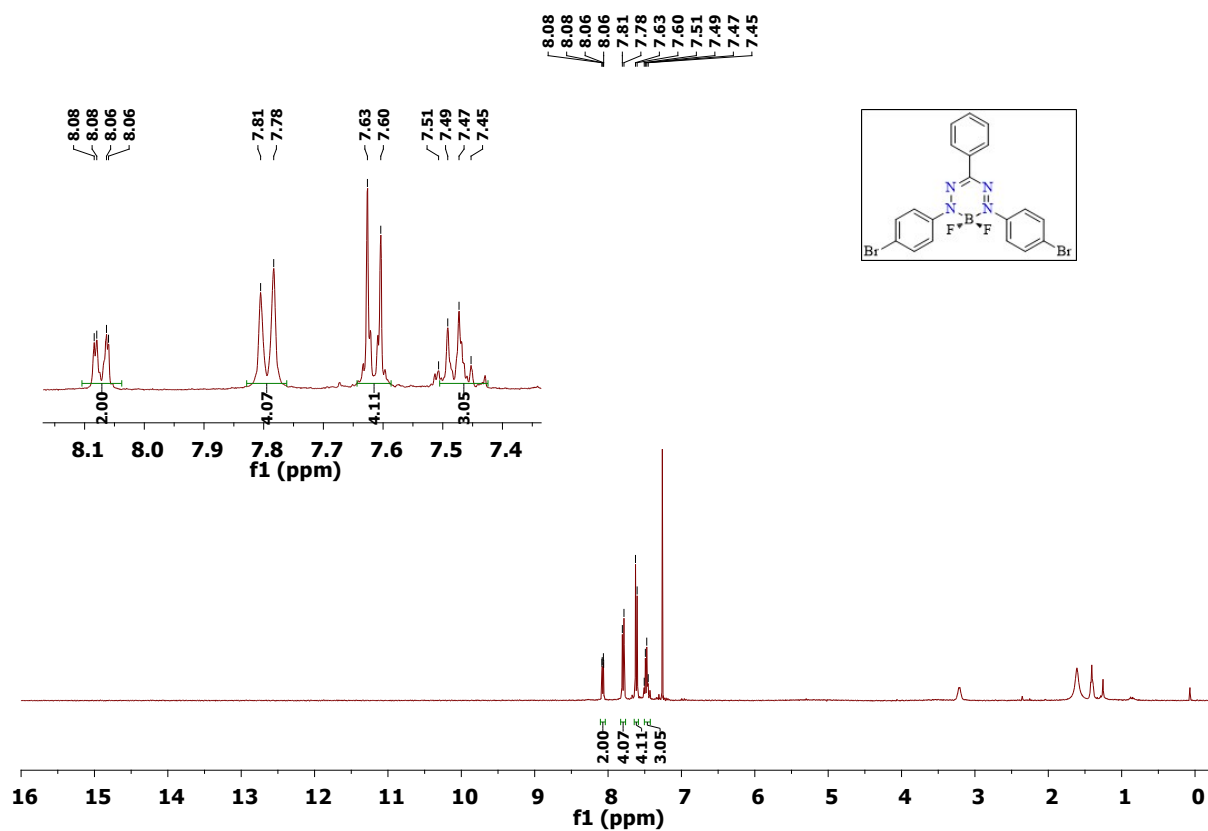


Fig. S6 <sup>1</sup>H NMR spectra of compound 7

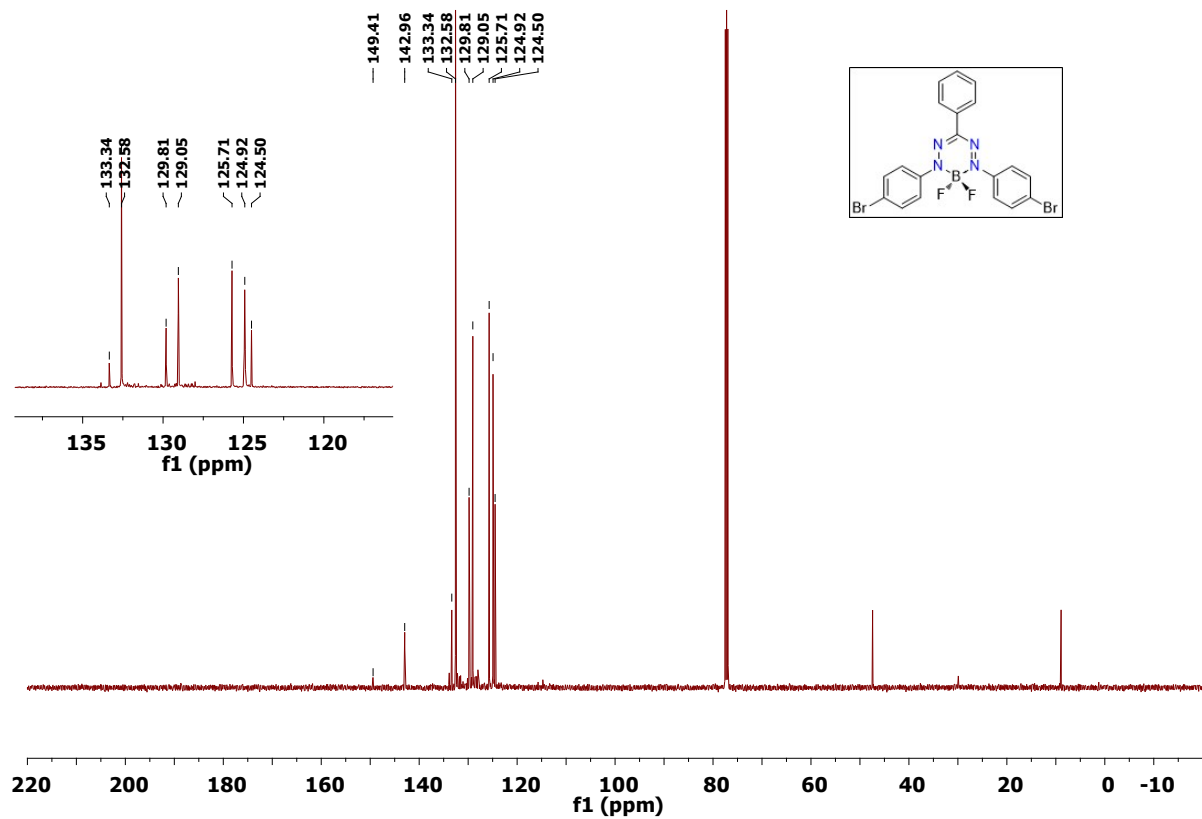


Fig. S7 <sup>13</sup>C NMR spectra of compound 7

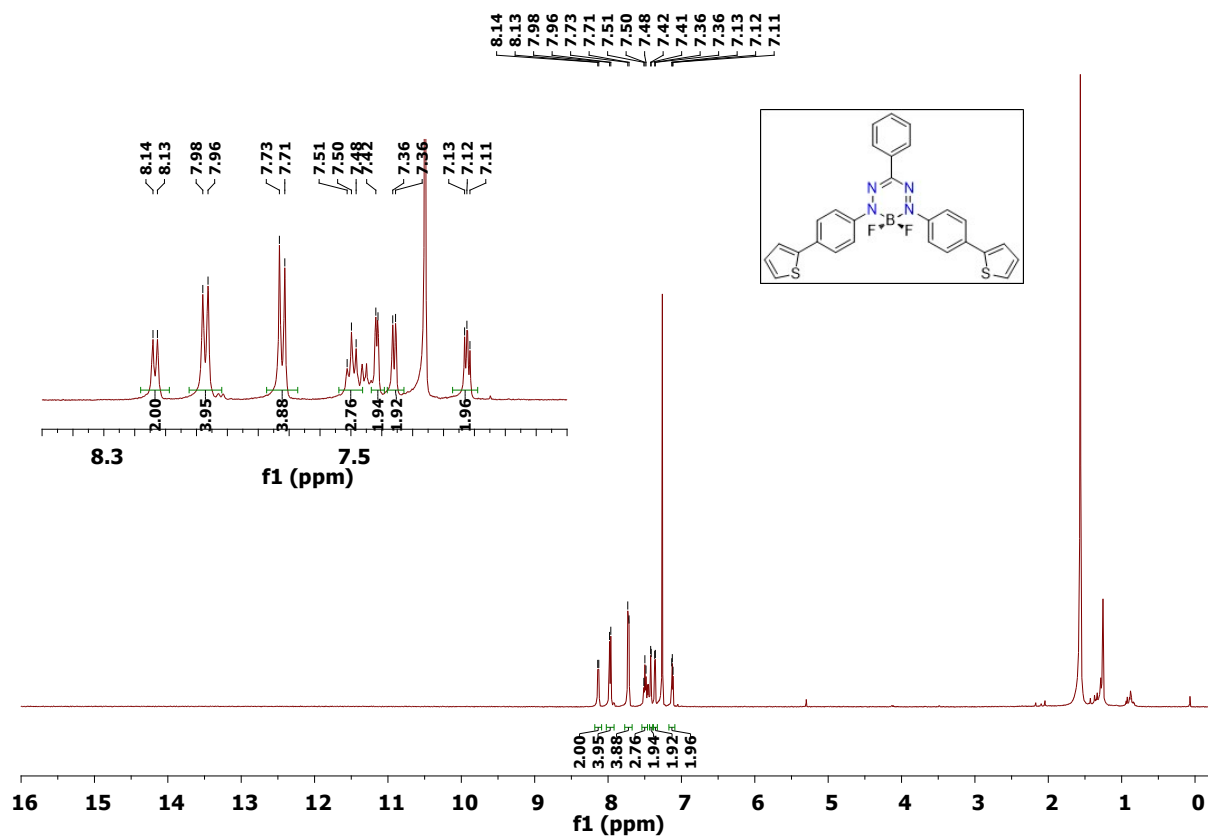


Fig. S8  $^1\text{H}$  NMR spectra of compound **8**

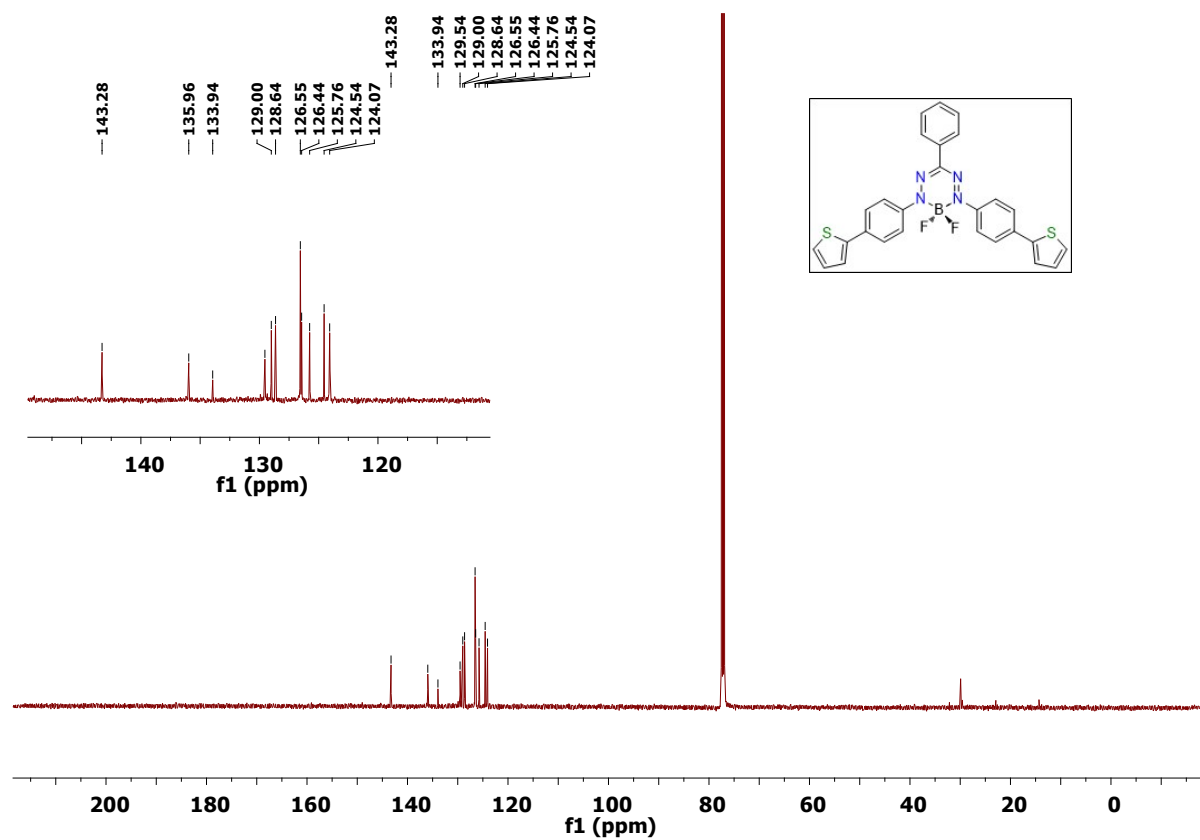


Fig. S9  $^{13}\text{C}$  NMR spectra of compound **8**

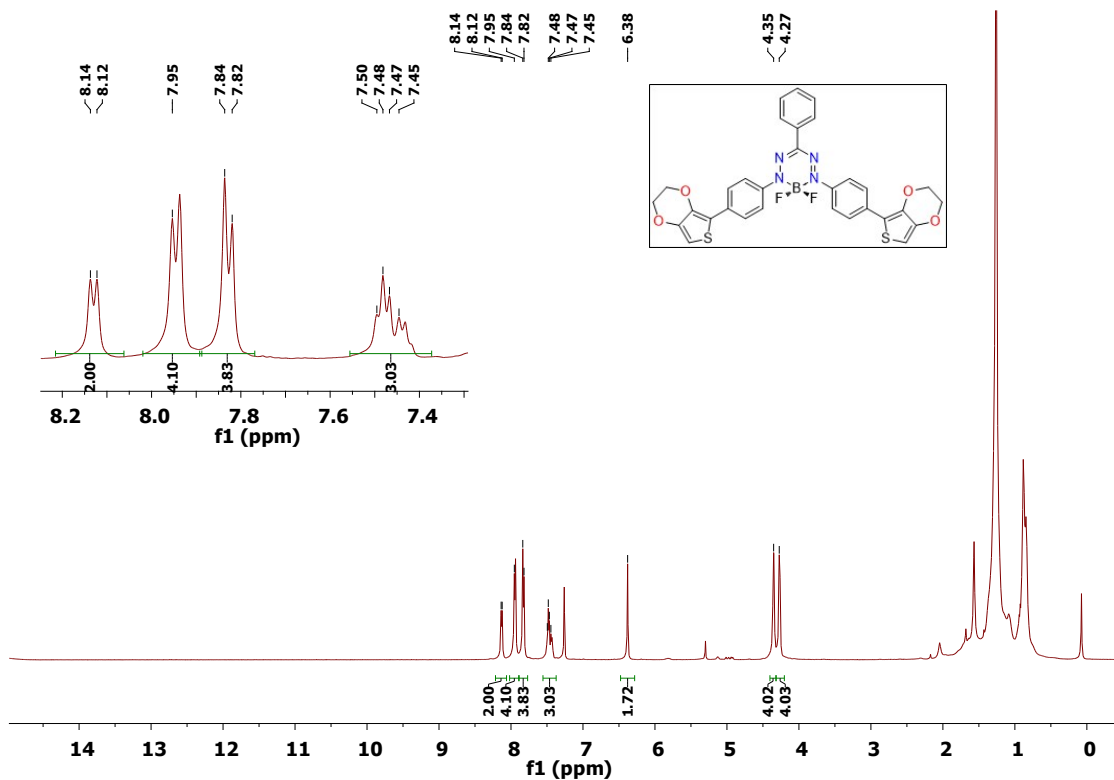


Fig. S10  $^1\text{H}$  NMR spectra of compound 9

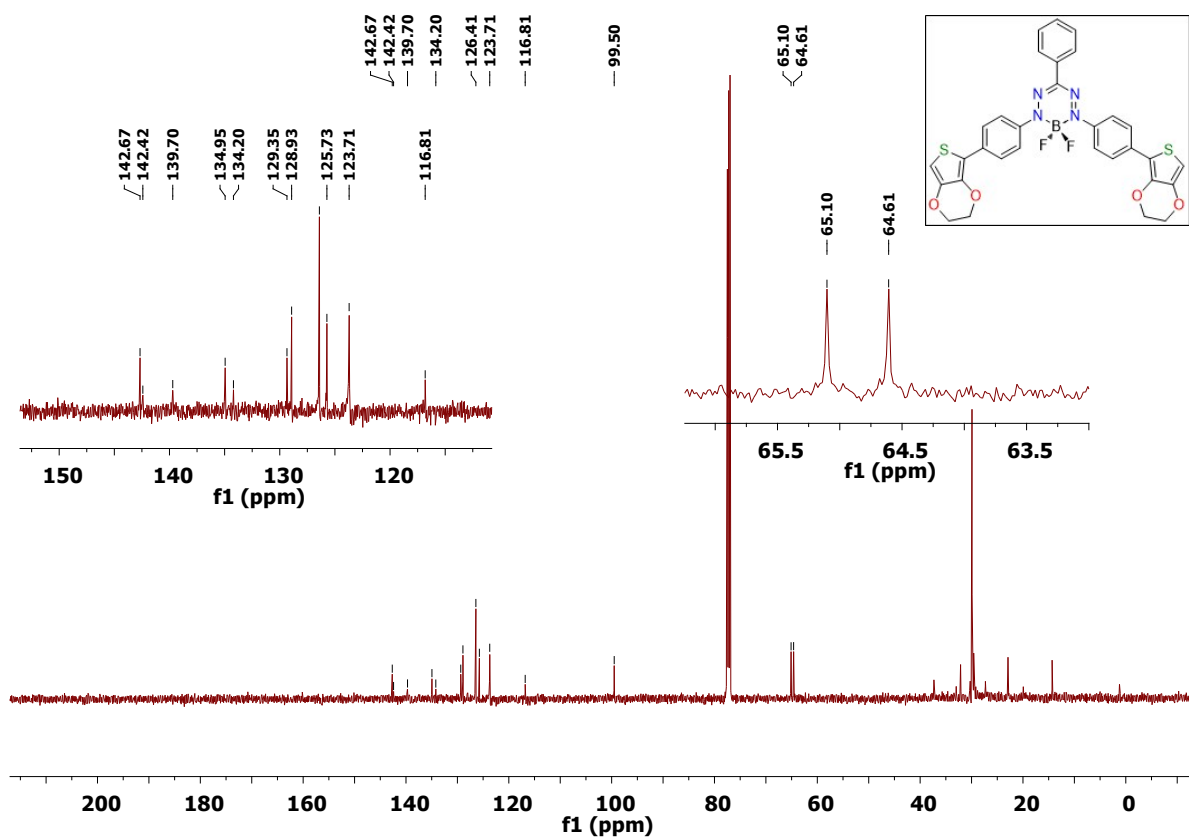


Fig. S11  $^{13}\text{C}$  NMR spectra of compound 9

## References

- 1 S. M. Barbon, J. T. Price, P. A. Reinkeluers and J. B. Gilroy, *Inorg. Chem.*, 2014, **53**, 10585–10593.
- 2 E. Kabir, C.-H. Wu, J. I.-C. Wu and T. S. Teets, *Inorg. Chem.*, 2016, **55**, 956–963.
- 3 S. M. Barbon, V. N. Staroverov and J. B. Gilroy, *J. Org. Chem.*, 2015, **80**, 5226–5235.
- 4 S. Pu, C. Zheng, Q. Sun, G. Liu and C. Fan, *Chem. Commun.*, 2013, **49**, 8036–8038.
- 5 S. S. Zhu and T. M. Swager, *J. Am. Chem. Soc.*, 1997, **119**, 12568–12577.
- 6 M. M. M. Raposo, A. M. C. Fonseca and G. Kirsch, *Tetrahedron*, 2004, **60**, 4071–4078.
- 7 O. V Dolomanov, L. J. Bourhis, R. J. Gildea, J. A. K. Howard and H. Puschmann, *J. Appl. Crystallogr.*, 2009, **42**, 339–341.
- 8 G. M. Sheldrick, *Acta Crystallogr. Sect. A*, 2008, **64**, 112–122.
- 9 M. J. Frisch, G. W. Trucks, H. B. Schlegel, G. E. Scuseria, M. a. Robb, J. R. Cheeseman, G. Scalmani, V. Barone, G. a. Petersson, H. Nakatsuji, X. Li, M. Caricato, a. V. Marenich, J. Bloino, B. G. Janesko, R. Gomperts, B. Mennucci, H. P. Hratchian, J. V. Ortiz, a. F. Izmaylov, J. L. Sonnenberg, Williams, F. Ding, F. Lipparini, F. Egidi, J. Goings, B. Peng, A. Petrone, T. Henderson, D. Ranasinghe, V. G. Zakrzewski, J. Gao, N. Rega, G. Zheng, W. Liang, M. Hada, M. Ehara, K. Toyota, R. Fukuda, J. Hasegawa, M. Ishida, T. Nakajima, Y. Honda, O. Kitao, H. Nakai, T. Vreven, K. Throssell, J. a. Montgomery Jr., J. E. Peralta, F. Ogliaro, M. J. Bearpark, J. J. Heyd, E. N. Brothers, K. N. Kudin, V. N. Staroverov, T. a. Keith, R. Kobayashi, J. Normand, K. Raghavachari, a. P. Rendell, J. C. Burant, S. S. Iyengar, J. Tomasi, M. Cossi, J. M. Millam, M. Klene, C. Adamo, R. Cammi, J. W. Ochterski, R. L. Martin, K. Morokuma, O. Farkas, J. B. Foresman and D. J. Fox, 2016, Gaussian 16, Revision C.01, Gaussian, Inc., Wallin.
- 10 K. Senthilkumar, F. C. Grozema, F. M. Bickelhaupt and L. D. A. Siebbeles, *J. Chem. Phys.*, 2003, **119**, 9809–9817.
- 11 E. F. Valeev, V. Coropceanu, D. A. da Silva Filho, S. Salman and J.-L. Brédas, *J. Am. Chem. Soc.*, 2006, **128**, 9882–9886.
- 12 S. I. Gorelsky, S. Ghosh and E. I. Solomon, *J. Am. Chem. Soc.*, 2006, **128**, 278–290.
- 13 J. Huang and M. Kertesz, *Chem. Phys. Lett.*, 2004, **390**, 110–115.
- 14 R. A. Marcus, *J. Chem. Phys.*, 1956, **24**, 966–978.
- 15 N. S. Hush, *J. Chem. Phys.*, 1958, **28**, 962–972.